





Clinicopathological findings of a long-term survivor of V180I genetic Creutzfeldt-Jakob disease

Yuichi Hayashi ^a, Yasushi Iwasaki ^b, Masahiro Waza ^c, Shinei Kato^a, Akio Akagi^b, Akio Kimura^a, Takashi Inuzuka^{a,d}, Katsuya Satoh^e, Tetsuyuki Kitamoto^f, Mari Yoshida^b, and Takayoshi Shimohata ^a

^aDepartment of Neurology, Gifu University Graduate School of Medicine, Gifu, Japan; ^bAutopsy Center of Prion Disease, Institute for Medical Sciences of Aging, Aichi Medical University, Nagakute, Japan; ^cDepartment of Neurology, Kakamigahara Rehabilitation Hospital, Kakamigahara, Japan; ^dDepartment of Neurology, Gifu Municipal Hospital, Gifu, Japan; ^eDepartment of Locomotive Rehabilitation Sciences, Nagasaki University Graduate School of Medicine, Nagasaki, Japan; ^fDivision of CJD Science and Technology, Department of Prion Research, Center for Translational and Advanced Animal Research on Human Diseases, Tohoku University School of Medicine, Sendai, Japan

ABSTRACT

The clinical characteristics of genetic Creutzfeldt-Jakob disease (gCJD) with a V180I mutation in the *PRNP* gene (V180I gCJD) are unique: elderly-onset, gradual progression, sporadic fashion, and cortical oedematous hyper-intensity on diffusion-weighted MRI (DW-MRI). This phenotype may become a potential target of future clinical therapeutic trials. The average disease duration of V180I gCJD patients is 23–27 months; however, considerably long-term survivors are also reported. The factors influencing survival and the clinicopathological characteristics of long-term survivors remain unknown. Herein, we report clinicopathological findings of a long-term survivor of V180I gCJD. A 78-year old woman was admitted to our hospital due to dementia and left hand tremor approximately 1.5 months after symptom onset. Neurological examination revealed dementia, frontal signs, and left hand tremor at admission. She had no family history of dementia or other neurological disease. DW-MRI revealed cortical oedematous hyper-intensities in the bilateral frontal lobes and the right temporal and parietal lobes. *PRNP* gene analysis indicated a V180I mutation with methionine homozygosity at codon 129. The symptoms gradually progressed, and she died of aspiration pneumonia 61 months after symptom onset. Neuropathological examination revealed severe cerebral atrophy with moderate to severe gliosis, but the brainstem was well preserved. Various-sized and non-confluent vacuole type spongiform changes were extensively observed in the cerebral cortices. Prion protein (PrP) immunostaining revealed weak and synaptic-type PrP deposits in the cerebral cortices. We consider that long-term tube feeding, and very mild brainstem involvement may be associated with the long-term survival of our V180I gCJD patient.

ARTICLE HISTORY

Received 19 October 2019
Revised 12 February 2020
Accepted 3 March 2020

KEYWORDS

V180I genetic Creutzfeldt-Jakob disease; diffusion-weighted MRI; long-term survivor; pathology; brainstem involvement

Introduction

Genetic Creutzfeldt-Jakob disease (gCJD) with a V180I mutation (V180I gCJD) in the *PRNP* gene is the most common type of gCJD in Japan, and accounts for 41.2% of gCJD patients [1]. Conversely, V180I gCJD is extremely rare in European countries, the United States, and China [2–4]. Its clinical characteristics are unique: elderly-onset, gradual progression, sporadic fashion, and cortical oedematous hyper-intensity on diffusion-weighted MRI (DW-MRI) [5,6]. Moreover, we previously reported unique single-photon emission computed tomography patterns such as preserve cerebral blood flow in the occipital cortices, brainstem, and cerebellum within the initial 2–3 years after disease onset [7]. The average disease duration of V180I gCJD patients is 23 or 27 months in methionine homozygote or M/V

heterozygote at codon 129 in the *PRNP* gene, respectively [6]. Long-term survivors whose disease duration is ≥ 5 -10 years have also been reported [8,9]; however, the influencing survival and the clinicopathological characteristics of long-term survivors of V180I gCJD remains unknown. Herein, we report the clinicopathological findings of a long-term survivor of V180I gCJD, and consider for a cause of the long-term survival.

Patient and methods

Clinical summary

A 78-year-old Japanese woman was admitted to our hospital due to a 1.5-month history of cognitive impairment and tremor in the left hand, without any family history of these symptoms. Neurological examination

revealed moderate cognitive impairment (15/30 points of the MMSE), left hand-tremor, bradykinesia, and parkinsonian gait, as described previously [7]. Cerebrospinal fluid (CSF) analysis revealed elevated levels of 14-3-3 protein and normal total tau protein levels. However, the prion proteins (PrP) in the CSF were not amplified by the real-time quaking-induced conversion method [10]. *PRNP* gene analysis revealed a V180I mutation with methionine homozygosity at codon 129. DW-MRI revealed cortical oedematous hyper-intensities in predominantly the right frontal and temporal lobes, excluding the basal ganglia, at 1.5 months after the onset (Figure 1a). We diagnosed the patient with V180I gCJD. Forced laughing was observed 9 months after the onset of symptoms; however, neither the startle response nor forced crying was observed during the disease course. DW-MRI acquired 9 months after the symptom onset revealed increased signals compared to the images taken 1.5 months after onset; the affected area exhibited bilateral expansion to the basal ganglia and parietal lobes (Figure 1b). Her symptoms gradually deteriorated to an akinetic mutism state by 14 months after onset, and she underwent tube feeding. The patient transferred to a chronic care hospital. Thereafter, we underwent long-term follow-up by our multidisciplinary medical network team for prion disease until death [11]. The symptoms gradually progressed, and the patient died of aspiration pneumonia 61 months after onset. DW-MRI performed 61 months after onset revealed that the cerebral atrophy had significantly progressed, and both the oedema and signal intensities in the bilateral cortices were diminished compared to those in images acquired 9 months after onset; however, hypertensive areas were observed in the bilateral basal ganglia (Figure 1c). We obtained informed consent to perform an autopsy from her family, and we transferred the patient's body to the Autopsy Centre of Prion Disease.

Neuropathological examination

A post-mortem study was performed 22.5 h after death. The brain, and upper cervical spinal cord were fixed in 20% neutral-buffered formalin for 4 weeks, and tissue blocks were immersed in 95% formic acid for 1 h to inactivate prion infectivity. The specimens were then embedded in paraffin and cut into 4- μ m sections. The sections were deparaffinized in lemosol, rehydrated through an ethanol gradient, and stained. For routine neuropathological examinations, sections were subjected to haematoxylin-eosin, Klüver-Barrera's (KB) and modified Gallyas-Braak silver stainings. Referring to the Iwasaki's pathological staging for sporadic

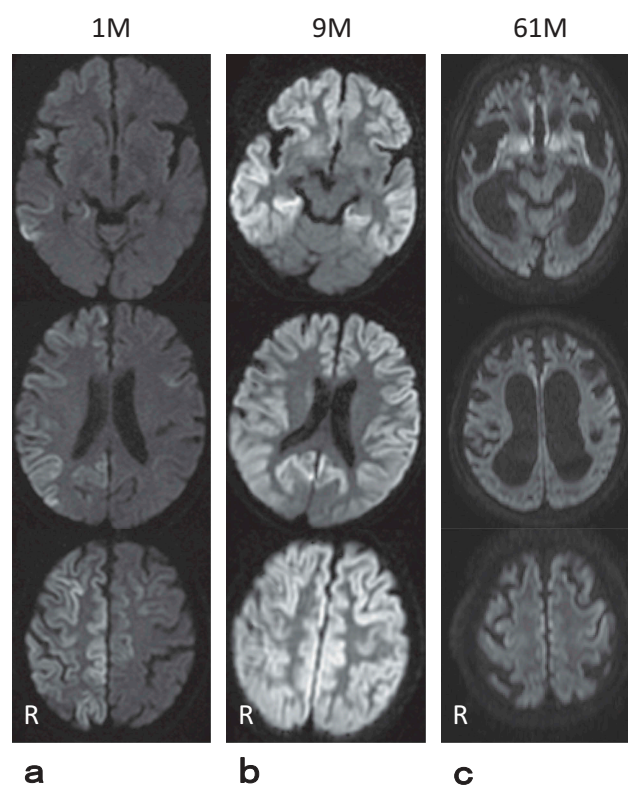


Figure 1. Serial diffusion-weighted MR images.

Diffusion-weighted MR images (DW-MRI) obtained from 1.5 (a), 9 (b), or 61 (c) months after disease onset, respectively. Panel a illustrates the cortical oedematous hyper-intensities observed predominantly in the right frontal and temporal lobes excluding basal ganglia, at 1.5 months after onset (a). DW-MRI performed 9 months after the onset exhibited increased signals compared to those on images acquired 1.5 months after onset; the affected area demonstrated bilateral expansion to the basal ganglia and parietal lobes (b). DW-MRI obtained 61 months after onset revealed that the cerebral atrophy had significantly progressed, and both oedema and signal intensities in the bilateral cortices were diminished compared to those on images taken 9 months after onset; however, hypertensive areas were observed in the bilateral basal ganglia (c).

CJD (sCJD) [12], we evaluated the severity of the neuropathological changes as mild, moderate or severe.

Immunohistochemical analysis was performed with a monoclonal antibody against PrP (3 F4; Dako, Glostrup, Denmark, mouse monoclonal, diluted 1:100) after hydrolytic autoclaving for antigen retrieval [13]. PrP immunostaining was conducted as previously described [14]. Immunostaining with anti-A β (4G8; Signet, Dedham, MA, mouse monoclonal, diluted 1:2,000), anti-hyperphosphorylated tau (AT-8; Innogenetics, Ghent, Belgium, mouse monoclonal, diluted 1:1,000), and anti-phosphorylated α -synuclein (pSyn#64; Wako Pure Chemical Industries, Osaka, Japan, mouse monoclonal, 1:3,000) was also performed. In these

immunostainings, primary antibody binding was detected using the envision amplified visualization method (En Vision plus kit; Dako). Peroxidase-conjugated streptavidin was visualized with 3, 3'-diaminobenzidine (DAB; Wako Pure Chemical Industries) as the final chromogen. Immunostained sections were lightly counterstained with Mayer's haematoxylin.

Western blot analysis of protease-resistant PrP

The cryopreserved right frontal cerebral cortex, which was snap frozen and stored at -80°C prior to use, was homogenized, and Western blot analysis of protease-resistant PrP was performed using 3F4 antibodies, as previously described [14].

Results

Macroscopic findings

The patient's brain weighed 920 g. Macroscopic analysis revealed severe diffuse cerebral atrophy predominantly in

the frontal and temporal lobes. No apparent atrophy was observed in the brainstem and cerebellum.

Microscopic findings

Moderate spongiform changes with neuropil rarefaction were extensively observed in the cerebral cortex, striatum and amygdala (Figure 2a,d). Morphologically, the spongiform changes consisted of various-sized and non-confluent vacuoles (Figure 2a,d). Severe gliosis and neuronal loss were recognized. Mild hypertrophic astrocytosis and ballooned neurons were also noted. However, the spongiform change in the precentral gyrus and the cortices of the occipital lobes were relatively milder than in those of the frontal and the temporal lobes (Figure 2c,g). The hippocampal formation, subiculum and parahippocampal gyrus were generally preserved with mild spongiform changes. The globus pallidus, lateral thalamus, and subthalamic nucleus were generally unaffected. The cerebral white matter exhibited mild myelin pallor with apparent gliosis. The spongiform changes and gliosis were mild in the cerebellar dentate nuclei, inferior olivary nuclei, and

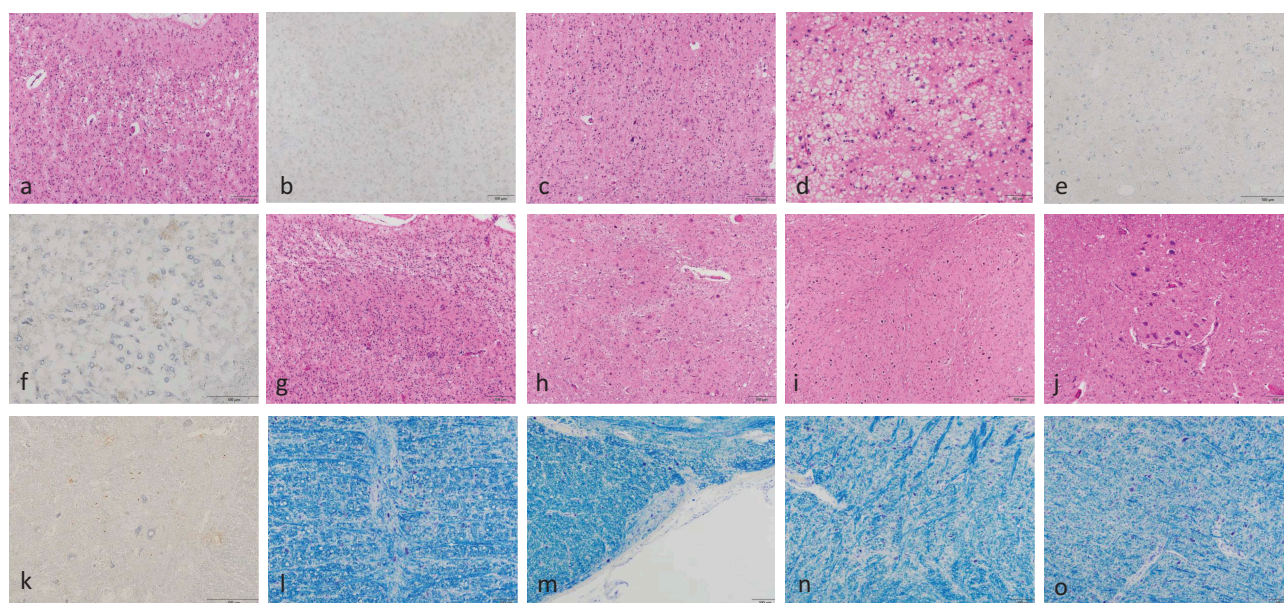


Figure 2. Microscopic findings.

Haematoxylin-eosin stains (A, C, D, G, H, I, J); anti-prion protein (PrP) immunostains using 3F4 antibodies (B, E, F, K); Klüver-Barrera's (KB) stains (L, M, N, O); the middle frontal gyrus (A, B); the precentral gyrus (C); the cortex of the amygdala (D, E); the subiculum (F); the striate area of the posterior lobe (G); the cerebellar dentate nuclei (H); the inferior olivary nuclei (I); the C3 level of the spinal cord (J, K); the obscure raphe nuclei (L), accurate nuclei of medulla oblongata (M), pre-Bötzinger complex (N), and dorsal respiratory group of the medulla (O). Moderate spongiform changes with neuropil rarefaction were extensively observed in the cerebral cortex, and the amygdala (a, d). The morphology of the spongiform changes showed various-sized and non-confluent vacuoles (a, d). Severe gliosis and neuronal loss were recognized. However, the spongiform changes in the precentral gyrus and the cortices of the occipital lobes were milder than in those of frontal and temporal lobes (c, g). The spongiform changes and gliosis were mild in the cerebellum dentate nuclei, inferior olivary nuclei, and upper cervical spinal cord (h, i, j). Anti-PrP immunostains were generally weak in the neocortices (b), amygdala (e), the subiculum (f), or upper cervical spinal cord (k). KB stains revealed preserved neurons in the obscure raphe nuclei (l), accurate nuclei of medulla oblongata (m), pre Bötzing complex (n), and dorsal respiratory group of the medulla (o).

upper cervical spinal cord (Figure 2h–j). The neurons were preserved in the raphe obscurus nuclei, accurate nuclei, pre-Bötzinger complex, and dorsal group in the KB stains (Figure 2l–o). In general, the brainstem, cerebellum and spinal cord were not severely involved as compared with cerebrum in this patient.

PrP immunohistochemical findings

PrP immunostaining revealed diffuse synaptic-type PrP deposits in the cerebral cortex, cerebellar cortex, and anterior and posterior horns of the spinal cord, but the immunoreactivity was generally weak (Figure 2b,e,f,k). PrP deposits were few in number in the medial temporal cortex and were partially enhanced in the senile plaques, particularly in the parahippocampal gyrus. No

PrP deposits were observed in the cerebral white matter or brainstem.

Ageing and accompaniment pathological findings

Ageing pathology was moderately observed. Neurofibrillary tangles (NFT) were found in the parahippocampus and entorhinal cortex and were determined to be Braak NFT stage II or AT8 NFT stage II (Figure 3a,b) [15]. The senile plaques were determined to be CERAD B, Braak stage B [15], and Thal phase 3/4 (Figure 3c,d) [16]. Alzheimer's disease pathology was mild according to the NIA-AA criteria [17]. Amyloid angiopathic change was evident. Argyrophilic grain was mild and was determined to be the Saito stage 1 [18]. Tufted astrocytes and astrocytic plaques were not

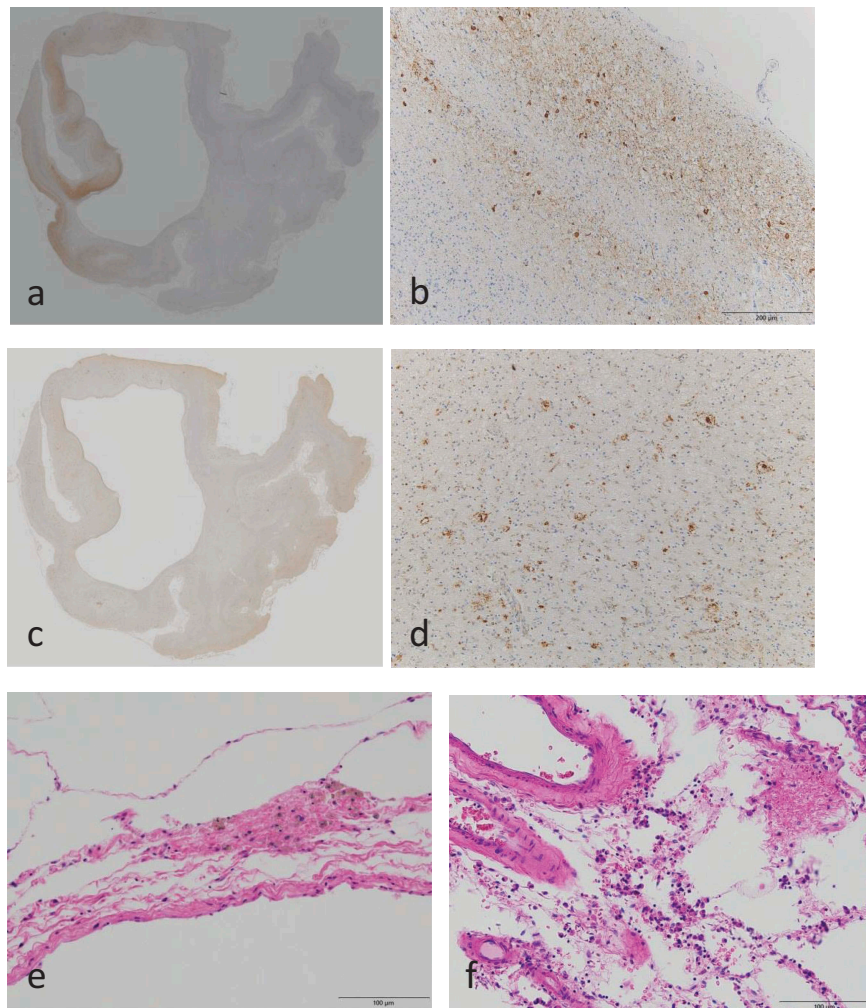


Figure 3. Ageing and accompaniment pathological findings.

AT8 stains (a, b); A β stains (c, d); Haematoxylin-eosin stains (e, f); the hippocampus (a, c); the entorhinal cortex (b); the calcarine sulcus (d); pia matter of the superior parietal lobule (e) and of the calcarine sulcus (f). Multiple micro-abscesses and inflammation changes in the pia matter were found (e, f)

found. Brain calcification was not found in the basal ganglia.

Multiple micro-abscesses and inflammation changes in the pia matter were found in the cerebrum, cerebellum, brainstem and spinal cord (Figure 3e,f). These infectious changes were secondary caused by severe aspiration pneumonia and the terminal stage of sepsis.

Findings of the Western blot analysis

The characteristic glycoform pattern of V180I gCJD [19] was also observed in the current patient. No diglycoform band (upper glycoform) was detected. The molecular weight of the non-glycoform band (unglycosylated) was consistent with type 2 PrP, but was slightly higher than that characteristic of sCJD (Figure 4).

Discussion

We herein report a patient with V180I gCJD who survived for more than 5 years after disease onset. We focused on two clinicopathological characteristics associated with long disease duration: appropriate long-term care for dysphagia, and mild involvement of the brainstem.

First, we described the clinical findings of the patient. This patient presented with severe pseudobulbar paralysis by 14 months after the onset; thereafter, she received long-term tube feeding. However, respiratory and cardiac functions were preserved during her disease course. A previous report indicated that the survival period of tube-fed patients with sCJD is longer than that of patients who were not tube fed [20]. To understand the timing of starting tube-fed or total parenteral nutrition (TPN), we reviewed 14 patients with autopsy-confirmed V180I gCJD including the current patient (Table 1) [8,21–33]. Combined V180I and M232R gCJD patients were excluded from our review. The clinical information for receiving tube-fed or TPN was available for only four patients. Three patients received tube-fed, and one patient received TPN in the late stage of the disease. Average (range) months between symptom onset and starting tube-fed or TPN, or duration tube-fed or TPN were 19.3 (11–30), or 33 (2–80) months, respectively. Our patient also received appropriate long-term care with tube feeding, and this could be associated with her long disease duration.

Second, the pathological characteristics of the current patient included moderate spongiform changes, severe gliosis, and severe neuronal loss in the cerebral cortices. However, the brainstem involvement was very mild. To understand the absence or presence of brainstem involvement, we reviewed 14 patients with autopsy-confirmed

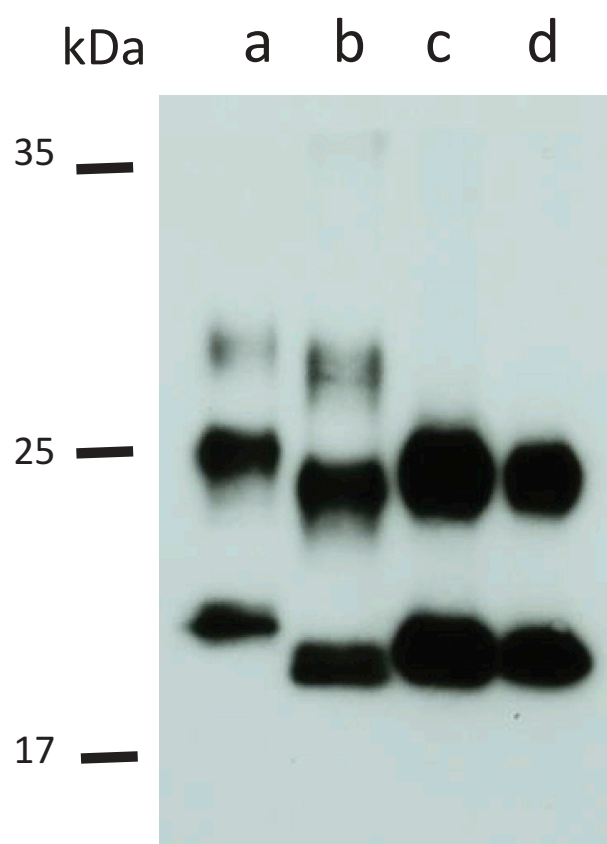


Figure 4. Western blot analysis of protease K-resistant prion protein.

Lane **a**: a control sample from the MM1 type of a sporadic Creutzfeldt-Jakob disease (sCJD) patient (6 fold diluted); lane **b**: a control sample from an MM2-cortical type of sCJD patient (25 fold diluted); lane **c**: a sample from the present patient (undiluted); lane **d**: a control sample from a V180I genetic Creutzfeldt-Jakob (gCJD) patient (undiluted). A characteristic glycoform pattern typical of V180I gCJD was observed in the current patient (**c**). No diglycoform band (upper glycoform) was detected. The molecular weight of the non-glycoform band (unglycosylated) was consistent with type 2 prion protein, but was slightly higher than that characteristic of sCJD (**c**).

V180I gCJD including the current patient (Table 1). The pathological findings in the brainstem were available for 11 of the 14 patients with V180I gCJD (Table 1). Ten of these 11 patients had mild or no involvement of the brainstem, regardless of disease duration. The remaining patient, who had received continuous intraventricular pentosane polysulfate infusion therapy, had numerous microspheres as well as PrP synaptic depositions in the central grey matter of the midbrain; however, medullar involvement was not described [28]. Moreover, Akagi, *et al* reported that the long-term survivors exhibited moderate spongiform changes regardless of disease duration, severe gliosis, and severe neuronal loss in the post-mortem analysis, and short-term survivors exhibited severe spongiform changes, moderate gliosis, and mild

Table 1. Clinicopathological findings of autopsy-verified V180I genetic Creutzfeldt-Jakob disease patients except for V180I/M232R combined patients.

Number	Author (y)	Onset of age (y)	Death of age (y)	Sex	Disease duration (mo.)	Initial symptom	Tube-fed or TPN (duration between onset and starting tube-fed orTPN) (mo.)	Brain weight (g)	Cerebral cortical involvement	Pathological brainstem involvement	Duration between onset and akinetic mutism
1	Matsumura (1995) [21]	77	79	F	25	Rt. Tremor	N.D.	1220	+	N.D.	18
2	Iwasaki (1999) [22], Akagi (2018) [8]	80	82	M	21	Rt. hemiparesis, motor aphasia	Oral intake until death	1060	+	Absent	9
3	Chassigneaux (2006) [23]	66	69	M	54	Dementia	N.D.	N.D.	+	Absent	12
4	Shindo (2006) [24]	79	84	F	61	Dementia, bradykinesia	N.D.	N.D.	+	Absent	N.D.
5	Suzuki (2008) [25], Suzuki (2009) [26]	79	80	M	13	Dementia	TPN (11)	3	2	+	+
6	Tsuboi (2009) [27], Honda (2013) [28]	64	70	F	72	Disorientation, memory deficit	N.D.	N.D.	+	Absent	N.D.
7	Yoshida (2010) [29]	77	79	F	26	Gait instability	N.D.	N.D.	+	Absent	18
8	Iwasaki (2011) [30], Akagi (2018) [8]	73	81	F	102	Aphasia	Tube-fed (22)	47	80	+	22
9	Yeo (2013) [31]	75	75	F	0.17	Semicoma	N.D.	N.D.	+	Absent	-
10	Iwasaki (2017) [32], Akagi (2018) [8]	78	81	F	33	Disorientation	Tube-fed (30)	3	3	+	16
11	Iwasaki (2018) [33], Akagi (2018) [8]	87	87	F	10	Slow reaction	Oral intake until death	N.D.	+	Absent	-
12	Akagi (2018) [8]	84	85	F	20	Numbness, tremor	N.D.	N.D.	+	Absent	5
13	Akagi (2018) [8]	73	81	F	101	Disorientation	N.D.	N.D.	+	Absent	20
14	Current patient	78	83	F	61	Lt. tremor, dementia	Tube-fed (14)	14	47	+	14
AVG + SD [range]		76.4 ± 6.1 [64–87]	79.7 ± 5.2 [69–87]	F (11/14)	42.8 ± 32.8 [0.17–101]		19.3 ± 8.5 [11–30] (n = 4)		33.0 ± 37.7 [2–80] (n = 4)		14.9 ± 5.5 (n = 9)
Cause of death	Cortical hyperintensities on initial DW-MRI	Onset of age (y)	Death of age (y)	Sex	Disease duration (mo.)	Initial symptom	Tube-fed or TPN (duration between onset and starting tube-fed orTPN) (mo.)	Brain weight (g)	Cerebral cortical involvement	Pathological brainstem involvement	Duration between onset and akinetic mutism
Pneumonia	N.E.	76.4 ± 6.1 [64–87]	79.7 ± 5.2 [69–87]	F (11/14)	42.8 ± 32.8 [0.17–101]		19.3 ± 8.5 [11–30] (n = 4)		33.0 ± 37.7 [2–80] (n = 4)		14.9 ± 5.5 (n = 9)
Pneumonia	+	76.4 ± 6.1 [64–87]	79.7 ± 5.2 [69–87]	F (11/14)	42.8 ± 32.8 [0.17–101]		19.3 ± 8.5 [11–30] (n = 4)		33.0 ± 37.7 [2–80] (n = 4)		14.9 ± 5.5 (n = 9)
N.D.	N.D.	76.4 ± 6.1 [64–87]	79.7 ± 5.2 [69–87]	F (11/14)	42.8 ± 32.8 [0.17–101]		19.3 ± 8.5 [11–30] (n = 4)		33.0 ± 37.7 [2–80] (n = 4)		14.9 ± 5.5 (n = 9)
Respiratory failure	+	76.4 ± 6.1 [64–87]	79.7 ± 5.2 [69–87]	F (11/14)	42.8 ± 32.8 [0.17–101]		19.3 ± 8.5 [11–30] (n = 4)		33.0 ± 37.7 [2–80] (n = 4)		14.9 ± 5.5 (n = 9)
Lung abscess, Pneumonia	+	76.4 ± 6.1 [64–87]	79.7 ± 5.2 [69–87]	F (11/14)	42.8 ± 32.8 [0.17–101]		19.3 ± 8.5 [11–30] (n = 4)		33.0 ± 37.7 [2–80] (n = 4)		14.9 ± 5.5 (n = 9)
Pneumonia	+	76.4 ± 6.1 [64–87]	79.7 ± 5.2 [69–87]	F (11/14)	42.8 ± 32.8 [0.17–101]		19.3 ± 8.5 [11–30] (n = 4)		33.0 ± 37.7 [2–80] (n = 4)		14.9 ± 5.5 (n = 9)
Pneumonia	+	76.4 ± 6.1 [64–87]	79.7 ± 5.2 [69–87]	F (11/14)	42.8 ± 32.8 [0.17–101]		19.3 ± 8.5 [11–30] (n = 4)		33.0 ± 37.7 [2–80] (n = 4)		14.9 ± 5.5 (n = 9)
Respiratory failure	+	76.4 ± 6.1 [64–87]	79.7 ± 5.2 [69–87]	F (11/14)	42.8 ± 32.8 [0.17–101]		19.3 ± 8.5 [11–30] (n = 4)		33.0 ± 37.7 [2–80] (n = 4)		14.9 ± 5.5 (n = 9)
Cardiovascular collapse	+	76.4 ± 6.1 [64–87]	79.7 ± 5.2 [69–87]	F (11/14)	42.8 ± 32.8 [0.17–101]		19.3 ± 8.5 [11–30] (n = 4)		33.0 ± 37.7 [2–80] (n = 4)		14.9 ± 5.5 (n = 9)
Respiratory failure	+	76.4 ± 6.1 [64–87]	79.7 ± 5.2 [69–87]	F (11/14)	42.8 ± 32.8 [0.17–101]		19.3 ± 8.5 [11–30] (n = 4)		33.0 ± 37.7 [2–80] (n = 4)		14.9 ± 5.5 (n = 9)
Respiratory failure	+	76.4 ± 6.1 [64–87]	79.7 ± 5.2 [69–87]	F (11/14)	42.8 ± 32.8 [0.17–101]		19.3 ± 8.5 [11–30] (n = 4)		33.0 ± 37.7 [2–80] (n = 4)		14.9 ± 5.5 (n = 9)
Respiratory failure	+	76.4 ± 6.1 [64–87]	79.7 ± 5.2 [69–87]	F (11/14)	42.8 ± 32.8 [0.17–101]		19.3 ± 8.5 [11–30] (n = 4)		33.0 ± 37.7 [2–80] (n = 4)		14.9 ± 5.5 (n = 9)
Respiratory failure	+	76.4 ± 6.1 [64–87]	79.7 ± 5.2 [69–87]	F (11/14)	42.8 ± 32.8 [0.17–101]		19.3 ± 8.5 [11–30] (n = 4)		33.0 ± 37.7 [2–80] (n = 4)		14.9 ± 5.5 (n = 9)

(Continued)

Table 1. (Continued).

Cause of death	Cortical hyperintensities on initial DW-MRI	Initial DW-MRI performed after the onset (mo.)	CSF 14-3-3 protein ($\mu\text{g/ml}$)	CSF total tau-protein (pg/mL)	Polymorphism at the codon 129 in the <i>PRNP</i> gene	Brain weight (g)	Cerebral cortical involvement	Pathological brainstem involvement
Respiratory failure	N.E.	N.E.	N.E.	N.E.	M/M	600	+	Absent
Pneumonia, sepsis	+	1.5	+	-	M/M	920	+	Very mild involvement
	+	9.1 \pm 13.8 (n = 8)	+	+	M/M (10/14)	960 \pm 212 (n = 12)	+	Absent or very mild (10/11)

N.D.: not described; N.E.: not examined; DW-MRI: diffusion-weighted MR image, PrP: prion protein; y: year-old; mo.: months; h: hours; F: female; M: male; +: positive; -: negative; Rt: Right; Lt: Left.

neuronal loss in the cerebral cortices [8]. The pathological findings of the current patient revealed a pathological pattern typical of a long-term survivor. Thus, we consider that two clinicopathological characteristics associated with long disease duration exist: appropriate long-term care with tube feeding, and very mild involvement of the brainstem with moderate cerebral spongiform changes. Especially, our observational study shows pseudobulbar palsy is a main cause of dysphagia in a patient with V180I gCJD, and an appropriate long-term care with tube feeding is crucial for a long-term follow-up

To date, despite several clinical trials, no effective treatment has been discovered for human prion disease. The rarity, rapidity, and clinical heterogeneity of prion disease affects study enrolment and the ability to measure treatment outcomes [34]. Since V180I gCJD is a gradually progressing prion disease [6], we believe that this phenotype may become a potential target of clinical therapeutic trials for prion disease as well as MM2-cortical-type of sCJD [35]. Therefore, in the setting of clinical trials, a good understanding of the clinicopathological characteristics of a long-term survivor of V180I gCJD is required.

Disclosure statement

No potential conflict of interest was reported by the authors.

Funding

This work was supported by grants-in-aid from the Research Committee of Prion Disease and Slow Virus infection (for TK, YI, and KS), and from the Research Committee of Prion Disease Surveillance (for TK, KS, and TI), the Ministry of Health, Labour and Welfare of Japan.

ORCID

Yuichi Hayashi  <http://orcid.org/0000-0003-4048-3513>
 Yasushi Iwasaki  <http://orcid.org/0000-0002-0059-3104>
 Masahiro Waza  <http://orcid.org/0000-0002-1582-4745>
 Takayoshi Shimohata  <http://orcid.org/0000-0002-8788-9089>

References

- [1] Nozaki I, Hamaguchi T, Sanjo N, et al. Prospective 10-year surveillance of human prion diseases in Japan. *Brain*. 2010;133:3043–3057.
- [2] Kovac GG, Puopolo M, Ladogana A, et al. Genetic prion disease: the EUROCJD experience. *Hum Gent*. 2005;118:166–174.
- [3] Minikel EV, Vallabh SM, Lek M, et al. Quantifying prion disease penetrance using large population control cohorts. *Sci Transl Med*. 2016;8:322ra9.

- [4] Shi Q, Zhou W, Chen C, et al. The features of genetic prion diseases based on Chinese surveillance program. *PLoS One*. 2015;10:e0139552.
- [5] Jin K, Shiga Y, Shibuya S, et al. Clinical features of Creutzfeldt-Jakob disease with V180I mutation. *Neurology*. 2004;62:502–505.
- [6] Qina T, Sanjo N, Hizume M, et al. Clinical features of genetic Creutzfeldt-Jakob disease with V180I mutation in the prion protein gene. *BMJ Open*. 2014;4:e004968.
- [7] Hayashi Y, Yoshikura N, Takekoshi A, et al. Preserved regional cerebral blood flow in the occipital cortices, brainstem, and cerebellum of patients with V180I-129M genetic Creutzfeldt-Jakob disease in serial SPECT studies. *J Neurol Sci*. 2016;370:145–151.
- [8] Akagi A, Iwasaki Y, Mimuro M, et al. Pathological progression of genetic Creutzfeldt-Jakob disease with a PrP V180I mutation. *Prion*. 2018;12:54–62.
- [9] Shimizu H, Shiga Y, Matsumoto A, et al. Serial magnetic resonance images of a Creutzfeldt-Jakob disease patient with V180I mutation obtained over 10 years. *Rinsho Shinkeigaku*. 2013;53:235–238. [in Japanese with English abstract].
- [10] Atarashi R, Satoh K, Sano K, et al. Ultrasensitive human prion detection in cerebrospinal fluid by real-time quaking-induced conversion. *Nat Med*. 2011;17:175–178.
- [11] Hayashi Y, Inuzuka T. A multidisciplinary medical network approach is crucial for increasing the number of autopsies for prion disease [Reply to: how we increase the numbers of autopsies for prion diseases? A model system in Japan]. *J Neurol Sci*. 2017;377:95–96.
- [12] Iwasaki Y, Tastumi S, Mimuro M, et al. Relationship between clinical findings and progression of cerebral cortical pathology in MM1-type sporadic Creutzfeldt-Jakob disease: proposed sataging of cerebral cortical pathology. *J Neurol Sci*. 2014;341:97–104.
- [13] Kitamoto T, Shin RW, Doh-ura K, et al. Abnormal isoform of prion proteins accumulates in the synaptic structures of the central nervous system in patients with Creutzfeldt-Jakob disease. *Am J Pathol*. 1992;140:1285–1294.
- [14] Iwasaki Y, Yoshida M, Hashizume Y, et al. Clinicopathologic characteristics of sporadic Japanese Creutzfeldt-Jakob disease classified according to prion protein gene polymorphism and prion protein type. *Acta Neuropathol*. 2006;112:561–571.
- [15] Braak H, Braak E. Neuropathological staging of Alzheimer-related changes. *Acta Neuropathol*. 1991;82:239–259.
- [16] Thal DR, Rüb U, Orantes M, et al. Phases of Aβ-deposition in the human brain and its relevance for the development of AD. *Neurology*. 2002;58:1791–1800.
- [17] Hyman BT, Phelps CH, Ceach TG, et al. National institute on aging Alzheimer's association guidelines for the neuropathologic assessment of Alzheimer's disease. *Alzheimers Dement*. 2012;8:1–13.
- [18] Saito Y, Ruberu NN, Sawabe M, et al. Staging of Argyrophilic grains: an age-associated tauopathy. *J Neuropathol Exp Neurol*. 2004;63:911–918.
- [19] Xiao X, Yuan J, Haik S, et al. Glycoform-selective prion formation in sporadic and familial forms of prion disease. *PLoS One*. 2013;8:e58786.
- [20] Iwasaki Y, Akagi A, Mimuro M, et al. Factors influencing the survival period in Japanese patients with sporadic Creutzfeldt-Jakob disease. *J Neurol Sci*. 2015;357:63–68.
- [21] Matsumura T, Kojima S, Kuroiwa Y, et al. An autopsy-verified case of Creutzfeldt-Jakob disease with codon 129 polymorphism and codon 180 point mutation. *Rinsho Shinkeigaku*. 1995;35:282–285. [in Japanese with English abstract].
- [22] Iwasaki Y, Sone M, Kato T, et al. Clinicopathological characteristics of Creutzfeldt-Jakob disease with a PrP V180I mutation and M129V polymorphism on different alleles. *Rinsho Shinkeigaku*. 1999;39(8):800–806. [in Japanese with English abstract].
- [23] Chasseigneaux S, Haik S, Laffont-Proust I, et al. V180I mutation of the prion protein gene associated with atypical PrPSc glycosylation. *Neurosci Lett*. 2006;408(3):165–169.
- [24] Shindo K, Shimokawa C, Ohta E, et al. Autopsy-proven Creutzfeldt-Jakob disease with a Codon 180 mutation showing dissociation between diffusion-weighted magnetic resonance imaging and single-photon emission computed tomography findings. *Eur Neurol*. 1995;35(1):46–49.
- [25] Suzuki K, Matsumura N, Suzuki T, et al. A case of Creutzfeldt-Jakob disease with codon 129 polymorphism and codon 180 point mutation. *Nippon Ronen Igakkai Zasshi*. Japanese Journal of Geriatrics. 2008;45(1):107–111. [in Japanese with English abstract].
- [26] Suzuki K, Matsumura N, Suzuki T, et al. Creutzfeldt-Jakob disease with V180I mutation and senile plaque. *Geriatr Gerontol Int*. 2009;9:210–212.
- [27] Tsuboi Y, Doh-ura K, Yamada T. Continuous intraventricular infusion of pentosane polysulfate: clinical trial against prion diseases. *Neuropathology*. 2009;29:632–636.
- [28] Honda H, Ishii R, Hamano A, et al. Microsphere formation in a subtype of Creutzfeldt-Jakob disease with a V180I mutation and codon 129 MM polymorphism. *Neuropathol Appl Neurobiol*. 2013;39:844–848.
- [29] Yoshida H, Terada S, Ishizu H, et al. An autopsy case of Creutzfeldt-Jakob disease with a V180I mutation of the PrP gene and Alzheimer-type pathology. *Neuropathology*. 2010;30:159–164.
- [30] Iwasaki Y, Mori K, Ito M, et al. An autopsied case of V180I Creutzfeldt-Jakob disease presenting with paraencephalopathic-type pathology and a characteristic prion protein type. *Neuropathology*. 2011;31:540–548.
- [31] Yeo MJ, Lee SH, Lee SY, et al. Familial Creutzfeldt-Jakob disease with a mutation at codon 180 presenting with an atypical phenotype. *J Clin Neurosci*. 2013;20:180–182.
- [32] Iwasaki Y, Mori K, Ito M, et al. An autopsy case of Creutzfeldt-Jakob disease with a prion protein gene codon 180 mutation presenting with pathological laughing and an exaggerated startle reaction. *Neuropathology*. 2017;37:575–581.

- [33] Iwasaki Y, Kato H, Ando T, et al. Autopsy case of V180I generic Creutzfeldt-Jakob disease presenting with early disease pathology. *Neuropathology*. 2018;38:638–645.
- [34] Appleby BS, Connor A, Wang H. Therapeutic strategies for prion disease: a practical perspective. *Curr Opin Pharmacol*. 2019;44:15–19.
- [35] Hayashi Y, Iwasaki Y, Waza M, et al. Clinicopathological findings of an MM2-cortical-type sporadic Creutzfeldt-Jakob disease patient with cortical blindness during a course of glaucoma and age-related macular degeneration. *Prion*. 2019;13:124–131.